BOLETIN DE LA SOCIEDAD ESPAÑOLA DE
Cerámica y Vidrio
www.elsevier.es/bsecv

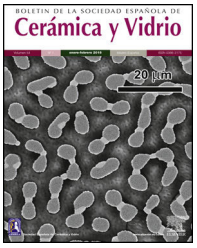

Original

Degradation of kaolinite clay added with Al_2O_3–Ta_2O_5 in H_2SO_4

José Alonso Valenzuela-Gutiérrez[a,*], *Alvaro González-Ángeles*[a], *Jorge López-Cuevas*[b]

[a] *Universidad Autónoma de Baja California, Facultad de Ingeniería, Blvd. Benito Juárez S/N, Mexicali B.C. 21280, Mexico*
[b] *CINVESTAV-IPN, Unidad Saltillo, Calle Industria Metalúrgica No. 1062, Parque Industrial Saltillo – Ramos Arizpe, Ramos Arizpe, CP 25900 Coahuila, Mexico*

ARTICLE INFO

Article history:
Received 3 April 2019
Accepted 17 July 2019
Available online 13 August 2019

Keywords:
Ceramic oxides
Sintering
Corrosion resistance

ABSTRACT

This study focuses on the degradation of kaolinite clay added with Al_2O_3 and Ta_2O_5, also known as tantite, to increase its resistance to an acid solution (H_2SO_4) at 300 °C. The samples tested for degradation were previously crushed, sieved, mixed, formed under cold isostatic pressing and sintered at 1150 °C. X-ray fluorescence (XRF) and X-ray diffraction (XRD) techniques were used to determine the composition and reveal the phases present in the samples. Degradation by static immersion (98 wt% H_2SO_4) was evaluated by the ASTM C267 mass loss technique. Predominant oxides of SiO_2, Al_2O_3 and Fe_2O_3 were found within the kaolinite clay, as well as other oxides in proportions lower than 2.39 wt%. The immersion of natural clay in sulfuric acid (at 300 °C) caused an increase in SO_3 content as well as in the mass of all samples. The X-ray diffractograms revealed the presence of quartz, cristobalite, curundum and tantite, as well as a significant reduction in their peak intensities after the interaction with H_2SO_4. The results showed that adding 20 wt% (sample M3C) and 40 wt% (sample M4C) of Ta_2O_5 to the kaolinite clay (sample M1C), produces a more stable structure and greater resistance to attack by H_2SO_4.

Degradación en H_2SO_4 de arcilla caolinítica adicionada con Al_2O_3–Ta_2O_5

Palabras clave:
Óxidos cerámicos
Sinterización
Resistencia a corrosión

RESUMEN

Se estudia la degradación de una arcilla caolinítica ante una solución ácida (H_2SO_4) a 300 °C, la cual fue adicionada con Al_2O_3 y Ta_2O_5, también conocida como tantita, para elevar la resistencia al ataque por la solución ácida. Las muestras sometidas a degradación fueron previamente trituradas, tamizadas, mezcladas, conformadas bajo compresión isostática en frío y sinterizadas a 1150 °C. Se utilizaron técnicas de fluorescencia de rayos X (XRF) y difracción de rayos X (DRX) para determinar la composición y revelar las fases presentes en las muestras. La degradación por inmersión estática (H_2SO_4 al 98% en peso) se evaluó a través de la técnica por pérdida de masa ASTM C267. En la arcilla caolinítica se encontraron óxidos

* *Corresponding author.*
E-mail address: avalenzuela18@uabc.edu.mx (J.A. Valenzuela-Gutiérrez).
https://doi.org/10.1016/j.bsecv.2019.07.004

predominantes de SiO_2, Al_2O_3 y Fe_2O_3, y otros óxidos en proporciones menores al 2.39% en peso. La inmersión en ácido sulfúrico (a 300 °C) ocasionó una elevación en el contenido de SO_3 y un incremento en la masa de todas las muestras. Los difractogramas de rayos X revelaron la presencia de cuarzo, cristobalita, corindón y tantita, así como una reducción significativa en la intensidad de los picos de todas estas fases después de la interacción con el H_2SO_4. Los resultados mostraron que al adicionar 20% y 40% en peso de Ta_2O_5 a la arcilla caolinítica (M1C), muestras M3C y M4C, respectivamente, se obtiene una estructura más estable y con mayor resistencia al ataque por H_2SO_4.

Introduction

Numerous publications agree that Ta_2O_5 is a good refractory material for some applications in furnaces, combustion equipment, etc. [1,2], even as a ceramic coating [3,4], because of its high chemical stability when immersed in acid solutions, particularly H_2SO_4, even in concentrations of 98 wt% [5]. It is widely used in the chemical industry as a coating to protect surfaces from reducing atmospheres [6]. It is known that chemical stability of pure ceramic materials or alloys subjected to acid solutions depends on the aggressiveness of the acid medium, the alloying elements or components of the sample, and the temperature at which the events occur [7,8]. The degree of degradation suffered by Ta_2O_5 in acid solutions has been determined in multiple analysis [9–11]. Other studies evaluated alloys such as Ta_2O_5–Al_2O_3, which offer an optimum performance in contact with said acid solution [12]. The main objective when formulating Ta_2O_5–Al_2O_3 alloys or forming coatings with these oxides is to demonstrate their high resistance to degradation by acid solutions [13,14], without forming compound phases such as $AlTaO_4$ that require more energy for their conformation. Corrosion results have also been reported for tantalum and titanium oxide composites, showing that the higher the Ta_2O_5 content, the mass gain is reduced after contact with H_2SO_4. There are also corrosion results for alloys of tantalum and titanium, where the higher the content of Ta_2O_5 the lower the mass gain after its interaction with H_2SO_4 [8]. Evaluations carried out on corrosion resistance of Ta_2O_5–Al_2O_3 materials demonstrated their ability to develop a passivation behavior when immersed in an acid solution [9,14]. Other studies analyzed this behavior with the deposition of superficial layers of Ta_2O_5 on a metallic material base [15,16], but further studies are still required to determine the behavior of a ternary system such as SiO_2–Al_2O_3–Ta_2O_5 in contact with solutions of H_2SO_4.

Materials and methods

The tested samples (Table 1) were made up of Al_2O_3 with ≥98% purity and Ta_2O_5 with ≥99% purity, both commercial materials from Sigma–Aldrich. They also contained a proportion of kaolinite clay from the San Jorge mine, located in the state of Baja California, Mexico, which has been reported to be a kaolin deposit with a composition of 19.46 wt% Al_2O_3 and 59.4 wt% SiO_2 [17].

Table 1 – Mixtures of kaolinite clay, Al_2O_3 and Ta_2O_5.

Elements (wt%)	M1C	M2C	M3C	M4C
Kaolinite clay	100	80	60	40
Al_2O_3	0	20	20	20
Ta_2O_5	0	0	20	40

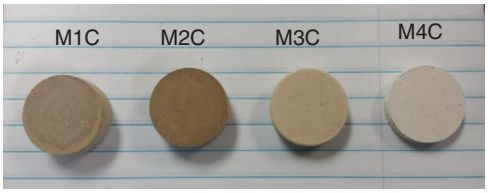

Fig. 1 – Cylindrical samples formed by cold isostatic pressing and sintered at 1150 °C.

Ten kilograms of kaolinite clay were mined from the San Jorge Mine with less than 25.40 mm in size [17], and then reduced to the test size by the ASTM-702 method using a mechanical sample separator. The clay was milled for 24 h in a high energy ball mill until obtaining a particle size of ≤75 μ, using a ball-to-powder weight ratio of 10 to 1, and mechanically sieved in a Ro Tap agitator model RX-29-9 following standard ASTM C-136.

The homogeneous mixing of the kaolinite clay, Al_2O_3 and Ta_2O_5, is a factor of high importance; therefore, a mechanical agitator was used. Also, cylindrical samples (50 mm diameter × 25 mm height) were formed by cold isostatic pressing at 27 MPa with an hydraulic press Carver series M3853, see Fig. 1 [18].

The densification of the samples (kaolinite clay with and without added Al_2O_3 and Ta_2O_5), Table 2, was developed under solid-state reaction synthesis, thermally treating them at 1150 °C/2 h [19] in a Sentro Tech furnace, with a heating rate of 5 °C/min [20].

To determine the chemical stability of the samples, a corrosion resistance test was carried out by a static immersion method [21,22]; the analysis was focused on assessing the degradation caused by sulfuric acid, through the method of mass loss established by the standard ASTM C-267 [23,24].

To evaluate the mass loss by immersion, each sample was submerged individually in 60 ml of acid solution (98 wt% H_2SO_4) inside a sealed Erlenmeyer flask. The experiment was carried out at 300 °C in a lab muffle furnace for a period of 6 days, as shown in Table 2.

Table 2 – Description of the acid solution and bulk density.

Acid solutions (98 wt%)	H_2SO_4, pH = 0.3			
Period of days	6			
Samples	M1C	M2C	M3C	M4C
Weight before sintering (g)	15.0771	14.5164	18.909	22.126
Boiling temp (°C)	300	300	300	300

Subsequently, the samples were removed from the acid solution and exposed to a drying cycle for 24 h. The mass in each sample was recorded before and after the corrosion test using a SCIENTECH ZSA 210 precision analytical scale.

The composition of the kaolinite clay and clay mixtures added with Al_2O_3 and Ta_2O_5 was determined by X-ray fluorescence (XRF) spectrometry [25,26], using a Bruker equipment Model S4 PIONNER.

The phase analysis of the kaolinite clay M1C and that of the sintered M2C, M3C and M4C mixtures were carried out by X-ray diffraction (XRD) with a *Bruker AXS* diffractometer model *D8 Advance* using *Cu-Kα* radiation. The Rietveld refinement method was used to carry out the quantification of the phases.

All samples were observed by optical microscopy, as well as on an environmental scanning electron microscope (MEB), Philips XL30 ESEM, where they were analyzed by Energy-dispersive X-ray spectroscopy (EDS), before and after the acid attack.

The density of the sintered samples, without acid attack, was determined by the Archimedes' principle in water.

Results and discussions

The kaolinite clay without sintering reveals initial contents of $SiO_2 \leq 74.32$ wt% and $Al_2O_3 \leq 21.83$ wt%, with traces of other materials in smaller proportions. According to Gazulla et al. [27], among the phase changes that occur in a kaolinite clay there are intermediate transitions, which start with formation of metakaolin at 500 °C and conclude with mullite and cristobalite appearing as major phases at 1550 °C [28,29]. Although it is not decisive that the formation of mullite occurs at 1120, 1150 or 1200 °C [27,28], the sintering at 1150 °C of the kaolinite clay of this study, is in an area where the primary mullite phase begins to form [28], and quartz theoretically begins to disappear at 800 °C, which ends at 1200 °C [29]. However, the x-ray diffractograms of kaolinite clay showed a higher concentration of the quartz phase when sintering at 1150 °C. On the other hand, the detection of significant amounts of cristobalite phase is attributed to the high content of SiO_2 in the kaolinite clay [30,31].

The XRF analysis (Table 3) revealed a high increase of SO_3 content in all the samples after their immersion in H_2SO_4. This happened through a chemical decomposition that was activated by raising the temperature of H_2SO_4 and keeping it within an evaporation–condensation cycle [32,33], for fuel-free atmospheres [34]. Interactions between the acid solution and the mixtures formed with kaolinite clay and the added oxides (Al_2O_3 and Ta_2O_5), produced an average reduction of 57% in the alumina oxide content of the mixtures (Table 3). Also, the initial content of Fe_2O_3 registered a minimum reduction (27.55 wt%) in the mixture of kaolinite clay added with 20 wt% of Al_2O_3, as well as a maximum reduction (73.83 wt%) when 40 wt% of Ta_2O_5 was added, after subjecting it to the attack by H_2SO_4. It is necessary to emphasize that the reduction in the amount of the iron and alumina oxides by immersion in H_2SO_4 is a behavior that has been reported in previous studies. It is known that the acid solution is effective decreasing the Al_2O_3 and Fe_2O_3 concentrations [35,36]. This effect is consistent with the results shown in Table 3. In the samples analyzed by XRF, weight losses due to ignition (LOI) are observed. Ignition losses of ≤0.24 wt% correspond to samples sintered at 1150 °C, without interaction with the acid solution. These losses occur mainly due to the dehydroxylation of kaolinitic clay or to the oxidation of organic matter. The samples sintered at 1150 °C, and with interaction with H_2SO_4, show high weight losses of 20.50 ≥ 31.10 wt% due to ignition, which are considered to also occur by dehydroxylation, but due to a high content of water molecules that were incorporated into the sample during the decomposition of H_2SO_4 at 300 °C [37,38].

The measured apparent densities were 2.65, 2.82, 3.28 and 3.91 g/cm^3, for sintered samples M1, M2, M3 and M4, respectively, without acid attack. This reflects the increment in the content of Ta_2O_5 and the diminution in the content of SiO_2, which occur simultaneously in the materials following the same order. Since all samples were formed using cold isostatic pressing, it was estimated that in all cases the porosity level was very small (maximum ~1%).

All samples subjected to H_2SO_4 increased their mass by forming passive compound layers [10,39], which are visible on the surfaces of the samples as small spots of similar distribution, see Fig. 2 [40]. It is considered that the spots of pink color revealed in the samples correspond in greater proportion to the formation of sulfates of Fe, Al and Si. The relative amount

Table 3 – Chemical composition of clay and mixtures determined by XRF.

Composition (wt%)	M1		M2		M3		M4	
	Before H_2SO_4	After H_2SO_4	Before H_2SO_4	After H_2SO_4	Before H_2SO_4	After H_2SO_4	Before H_2SO_4	After H_2SO_4
Ta_2O_5	N/R	N/R	N/R	N/R	44.04	25.59	48.08	43.09
SiO_2	68.34	44.49	48.81	25.31	32.44	14.80	27.70	13.25
SO_3	0.474	16.22	0.156	19.02	0.215	18.01	0.19	9.95
Al_2O_3	22.88	12.56	42.42	21.57	20.88	14.29	22.42	12.16
Fe_2O_3	4.97	2.89	5.833	1.607	1.548	0.925	0.837	0.618
Others	3.239	2.329	2.642	1.182	0.780	0.736	0.499	0.391
LOI	0.075	21.50	0.120	31.10	0.070	25.60	0.240	20.50

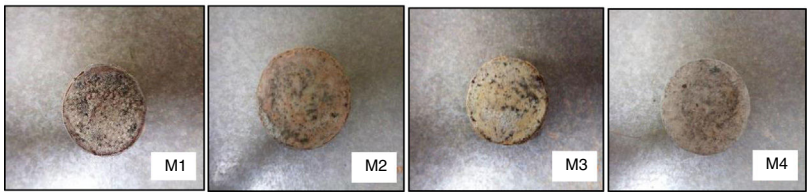

Fig. 2 – Optical macrographs of samples with small spots of similar distribution.

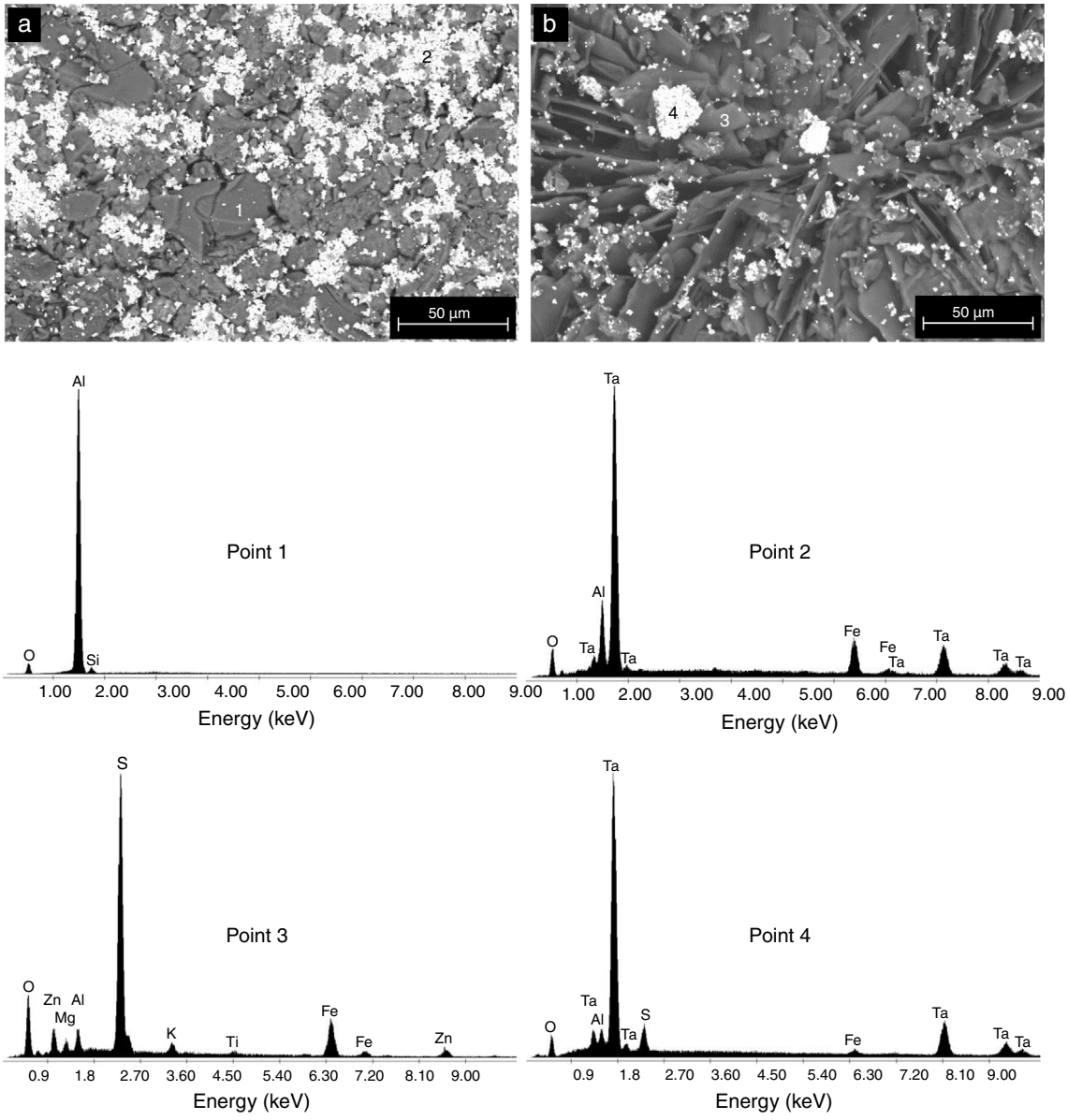

Fig. 3 – SEM micrographs of sample M4C, before (a) and after (b) subjecting it to the attack by H_2SO_4. The EDS spectra of the analyzed points are also shown.

of the formed sulfates decreased in this order, since the Fe ions are altered to a greater extent than the Al ions [41,42].

The formation of $Al_2(SO_4)_3$, $Ta_2(SO_4)_5$, $FeSO_4$, and possibly also $Si(SO_4)_2$, during the attack with H_2SO_4 given to the kaolinite clay added with Al_2O_3 and Ta_2O_5, was confirmed by the analyzes of SEM/EDS performed, see Fig. 3. Probably these phases were not detected by XRD due to their relatively small amount. The SEM micrographs (Fig. 3a and b) showed that the surface of the samples changed completely as a result of the acid attack, from a polycrystalline microstructure typical of a sintered material, in which the presence of a large quantity of agglomerates of very fine Al_2O_3 and Ta_2O_5 particles are clearly

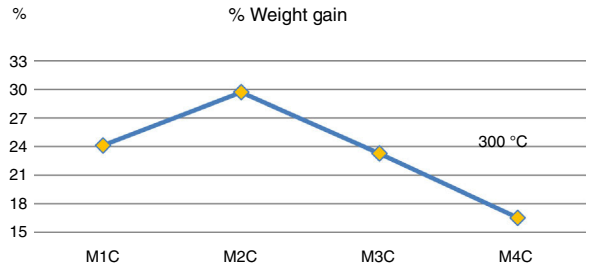

Fig. 4 – Weight gains in the clay mixtures in 98 wt% H_2SO_4 solution at 300 °C.

seen, to a microstructure formed by a mixture of sulphates with plate-like morphology, with large hollow spaces formed between them due to the partial dissolution of the matrix, and with the presence in the attacked sample of a relatively small amount of unreacted Al_2O_3 and Ta_2O_5 remaining.

Fig. 4 shows mass increases after 6 days of immersion in H_2SO_4. It is observed that the addition of 20 wt% (sample M3C) and 40 wt% (sample M4C) of Ta_2O_5 to the kaolinite clay (sample M1C), which is composed basically of SiO_2 and Al_2O_3, produced the lowest mass gain due to the interaction with the acid solution. This behavior indicates that the passive layers produced by the addition of Ta_2O_5 had a greater resistance to H_2SO_4 than kaolinite clay. And when 20 wt% of Al_2O_3 was added to the kaolinite clay (sample M1C), it produced the highest mass increase compared to the rest of the samples. Other studies have recorded favorable yields combining Al_2O_3–Ta_2O_5 and subjecting them to acid solutions [14], as well as by increasing the content of Ta_2O_5 in the mixtures [8].

The X-ray diffractograms of Figs. 5–8 revealed a significant decrease in the intensity of the diffraction peaks after subjecting the samples to the acid solution. This indicates that the crystalline structure of quartz, cristobalite, corundum and tantite [43] partially collapsed or became amorphous after immersion in H_2SO_4, or that the crystalline structure of kaolinite clay added with alumina and tantalum oxide partially collapsed or became amorphous after immersion in H_2SO_4 [9].

Figure 5 shows the X-ray diffractogram of sample M1C, for which 92.2 wt% quartz (predominant phase) and 6.9 wt% cristobalite (minor phase) was recorded before immersion of the sample in H_2SO_4. After immersion in H_2SO_4, the peak intensity was reduced for quartz, but cristobalite reacted to a greater extent, which almost caused its complete disappearance in the samples [43,44]. Lastly, the X-ray diffractograms of

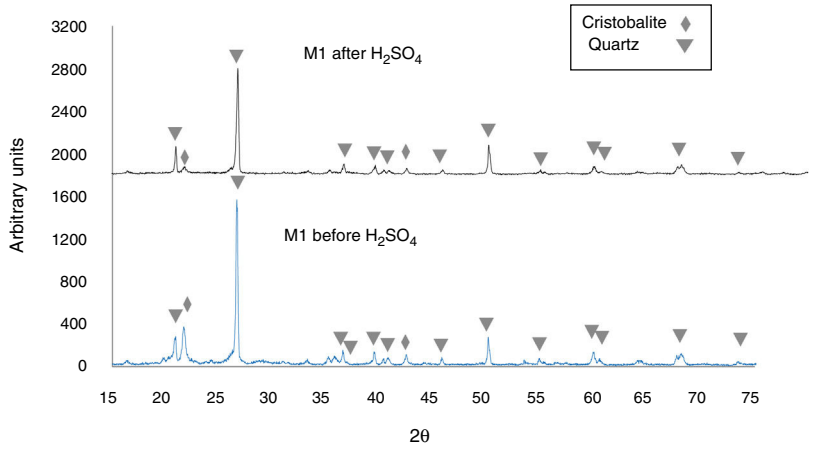

Fig. 5 – XRD of kaolinite clay before and after immersion in H_2SO_4 at 300 °C.

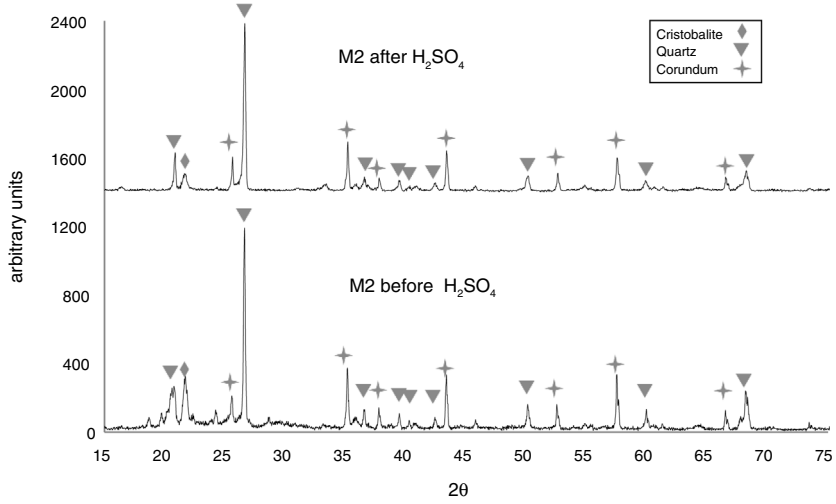

Fig. 6 – X-ray diffractograms of kaolinite clay with added Al_2O_3 before and after immersion in H_2SO_4 at 300 °C.

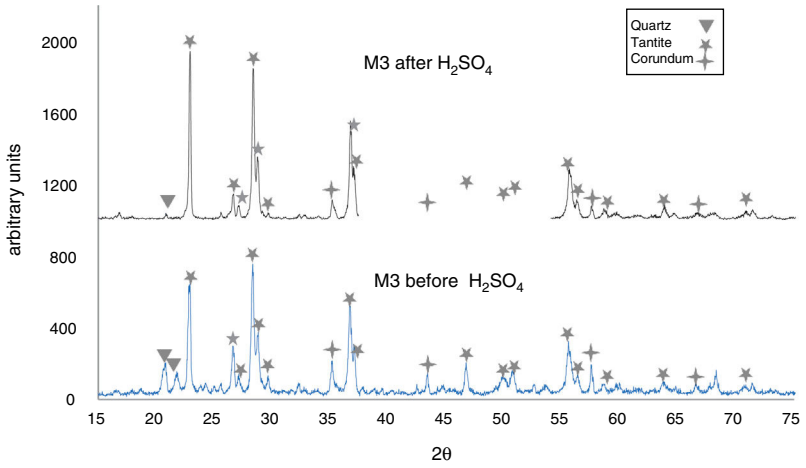

Fig. 7 – X-ray diffractograms of kaolinite clay with added Al_2O_3 and 20 wt% Ta_2O_5 before and after immersion in H_2SO_4 at 300 °C.

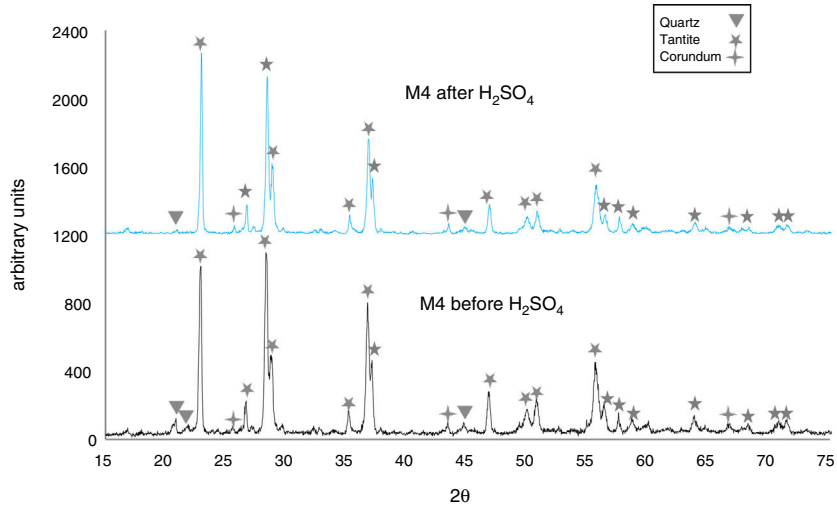

Fig. 8 – X-ray diffractograms of kaolinite clay with added Al_2O_3 and 40 wt% Ta_2O_5 before and after immersion in H_2SO_4 at 300 °C.

Fig. 5 show an amorphous "hump" overlapped with a cristobalite peak located at $2\theta = 21.8°$ [45,46], before immersion in the H_2SO_4, which indicates that an amorphous phase was formed during heat treatment of the sample. After the acid attack, this hump disappears, which was likely due to dissolution of the amorphous phase.

In Fig. 6, the X-ray diffractogram shows the presence of quartz (48 wt%), corundum (43.4 wt%), and cristobalite (4.2 wt%) phases in sample M2C, before its immersion in the acid solution. The peak intensity of the cristobalite phase was again drastically reduced, after interacting with sulfuric acid.

The X-ray diffractograms of Figs. 7 and 8 of materials of the SiO_2–Al_2O_3–Ta_2O_5 system did not reveal the formation of new phases, considering that the reactions occurred in the subsolid region of Ta_2O_5 at 1150 °C [47]. It is also likely that the solubility limit between Ta_2O_5 and Al_2O_3 was not exceeded in the solid-solid region, due to the absence of the $AlTaO_4$ phase [12,48]. The interactions of the acid solution with the tantite (Ta_2O_5) [49] and corundum phases resulted in significant reductions in their peak intensities after their immersion in H_2SO_4. However, the interaction between the acid medium and the quartz phase, reduced its peak intensities almost completely. This may mean that the proportion of these phases decreases in the samples as a consequence of the attack by the acid solution, either because they react with the acid to form sulfates, or because they become dissolved into the solution.

Conclusions

The present study was focused on the degradation of kaolinite clay with added Al_2O_3 and Ta_2O_5 to increase its resistance to an acid solution (H_2SO_4) at 300 °C. Based on the reported results and their implications, the following conclusions can be drawn:

- Exposure to 98 wt% H_2SO_4 at 300 °C produced a high increase in the SO_3 content of kaolinite clay samples with added alumina and tantalum oxide, due to the chemical

decomposition of H_2SO_4 activated by increasing the temperature above its boiling point.
- Addition of alumina and tantalum oxide to kaolinite clay, in proportions of 20 wt% and 20–40 wt%, respectively, develops passive layers with better resistance to the acid solution.
- In all X-ray diffractograms of Figs. 5–8, a severe decrease in the intensity of the peaks of the cristobalite phase was detected as a result of the interaction with H_2SO_4, indicating that this is the least stable phase in the mixture.
- None of the X-ray diffractograms obtained in this work revealed the formation of new crystalline phases when the kaolinitic clay added with Al_2O_3 and Ta_2O_5 was sintered at 1150 °C.

Author contribution statement

A. Valenzuela-Gutiérrez wrote the draft paper, got the raw materials and synthesized the studied samples.

A. González-Ángeles ensures that all authors are included in the author list, its order has been agreed by all authors, and that all authors are aware that the paper was submitted.

J. López-Cuevas made the characterization of samples and supervised the final manuscript.

Conflict of interest statement

The authors declare that they have no conflict of interest.

Acknowledgements

Authors are greatly grateful to the Universidad Autónoma de Baja California and CINVESTAV-Saltillo for facilitating access and use of their facilities and equipment to carry out this research.

REFERENCES

[1] J.B. Lambert, Refractory metals and alloys, Prop. Sel. Alloy. Spec.-Purpose Mater. 2 (July 2015) (1990) 557–585.
[2] S. Zlotnik, A. Tkach, P.M. Vilarinho, Functional tantalum-based oxides: from the structure to the applications, Adv. Ceram. (2016) 337–383.
[3] W.B.B. Rahmati, A. Sarhan, Ceramic tantalum oxide thin film coating to enhance the corrosion and wear characteristics of Ti–6Al–4V alloy, J. Alloys Compd. (12) (2016) 4908–4911.
[4] W. Hu, et al., Corrosion and wear behaviours of a reactive-sputter-deposited Ta_2O_5 nanoceramic coating, Appl. Surf. Sci. 368 (2016) 177–190.
[5] A. Robin, M.E. de Almeida, C.A. Nunes, Corrosion behavior of niobium and Nb–25 wt% Ta alloy in sulfuric acid solutions, Corrosion 47 (6) (1991) 443–448.
[6] P. Shang, S. Xiong, L. Li, D. Tian, W. Ai, Investigation on thermal stability of Ta_2O_5, TiO_2 and Al_2O_3 coatings for application at high temperature, Appl. Surf. Sci. 285 (Part B) (2013) 713–720.
[7] C. Sio, A.O. Mgo, Effects of temperature, refractory composition and mass transfer rate on corrosion rate of Al_2O_3–SiO_2 system bricks into, ISIJ Int. 57 (4) (2017) 697–705.
[8] Y.L. Zhou, M. Niinomi, T. Akahori, H. Fukui, H. Toda, Corrosion resistance and biocompatibility of Ti–Ta alloys for biomedical applications, Mater. Sci. Eng. A 398 (1–2) (2005) 28–36.
[9] G.S. Frankel, et al., A comparative review of the aqueous corrosion of glasses, crystalline ceramics, and metals, NPJ Mater. Degrad. 2 (1) (2018) 15.
[10] A. Ertan, CO_2 and N_2 adsorption on the acid (HCl, HNO_3, H_2SO_4 and H_3PO_4) treated zeolites, J. Mater. Sci. 34 (4) (2005) 151–156.
[11] A. Robin, Corrosion behavior of niobium, tantalum and their alloys in boiling sulfuric acid solutions, Int. J. Refract. Met. Hard Mater. 15 (5–6) (1997) 317–323.
[12] J.E. Zhou, J. Zhang, X.Z. Zhang, X.B. Hu, Effect of Al_2O_3 addition on microstructure, thermal expansion and mechanical properties of Ta_2O_5 ceramics, Key Eng. Mater. 512 (2012) 631–634.
[13] E. Salmi, Atomic Layer Deposited Coatings for Corrosion Protection of Metals, University of Helsinki Finland, 2015.
[14] N. Hara, S. Nagata, N. Akao, K. Sugimoto, Formation of Al_2O_3–Ta_2O_5 double-oxide thin films by low-pressure MOCVD and evaluation of their corrosion resistances in acid and alkali solutions, J. Electrochem. Soc. 146 (2) (1999) 510–516.
[15] W. Jin, et al., Corrosion resistance and cytocompatibility of tantalum-surface-functionalized biomedical ZK60 Mg alloy, Corros. Sci. 114 (2017) 45–56.
[16] A. Hee, Wear and corrosion resistance of tantalum coating on titanium alloys for biomedical implant applications, The University of Wollongong School of Mechanical, Materials Mechatronic and Biomedical Engineering (2017).
[17] M.C.J. Cobo, B. Valdez, Minerales Industriales Del Estado Peninsular De Baja California, México, 2010, pp. 3–14.
[18] C. Sadik, I.E. El Amrani, A. Albizane, Processing and characterization of alumina-mullite ceramics, J. Asian Ceram. Soc. 2 (4) (2014) 310–316.
[19] O. Aladesuyi, M. Pal, S.K. Das, K.O. Ajanaku, Phase and microstructural evolution during sintering of mixture of 75:25 Nigerian kaolin and calcined alumina powder compacts, J. Mater. Environ. Sci. 8 (Cvd) (2017) 2832–2838.
[20] J.A. Amkpa, N.A. Badarulzaman, A.B. Aramjat, Influence of sintering temperatures on physico-mechanical properties and microstructure of refractory fireclay bricks, Int. J. Eng. Technol. Influ. 8 (6) (2017) 2588–2593.
[21] S. Izquierdo, E. Rodríguez, R.M. De Gutiérrez, U. Valle, Resistance to acid corrosion of blended cements mortars with spent fluid catalytic cracking (sFCC) catalyst Resistencia a la corrosión ácida de morteros de cementos adicionados con catalizador de craqueo catalítico gastado (sFCC), Rev. Ing. Construcción RIC 30 (2015) 169–176.
[22] H.S.M. Mobin, Corrosion behavior of mild steel and SS 304L in presence of dissolved nickel under aerated and deaerated conditions, Mater. Res. 14 (4) (2011) 524–531.
[23] ASTM C267-01, Standard test methods for chemical resistance of mortars, grouts and monolithic, ASTM C267-01 04 (February) (1998) 1–6.
[24] M. Said-Mansour, E.H. Kadri, S. Kenai, M. Ghrici, R. Bennaceur, Influence of calcined kaolin on mortar properties, Constr. Build. Mater. 25 (5) (2011) 2275–2282.
[25] G. Shell, R.H. Additives, Open access enhancement of refractory properties of blended clay with, Am. J. Eng. Res. 6 (6) (2017) 218–226.
[26] A. Job Ajala, N.A. Badarulzaman, A.B. Aramjat, Impact of sintering temperatures on microstructure, porosity and mechanical strength of refractory brick, Mater. Sci. Forum 888 (2017) 66–70.
[27] M.F. Gazulla, M.P. Gómez, A. Barba, J.C. Jarque, Characterization of ceramic oxide refractories by XRF and XRD, X-ray Spectrom. 33 (6) (2004) 421–430.

[28] Y.F. Chen, M.C. Wang, M.H. Hon, Transformation kinetics for mullite in kaolin-Al_2O_3 ceramics, J. Mater. Res. 18 (6) (2003) 1355–1362.
[29] A.H. De Aza, X. Turrillas, M.A. Rodriguez, T. Duran, P. Pena, Time-resolved powder neutron diffraction study of the phase transformation sequence of kaolinite to mullite, J. Eur. Ceram. Soc. 34 (5) (2014) 1409–1421.
[30] C.Y. Chen, G.S. Lan, W.H. Tuan, Preparation of mullite by the reaction sintering of kaolinite and alumina, J. Eur. Ceram. Soc. 20 (14–15) (2000) 2519–2525.
[31] F. Sahnoune, M. Chegaar, N. Saheb, P. Goeuriot, F. Valdivieso, Algerian kaolinite used for mullite formation, Appl. Clay Sci. 38 (3–4) (2008) 304–310.
[32] D.M. Ginosar, H.W. Rollins, L.M. Petkovic, K.C. Burch, M.J. Rush, High-temperature sulfuric acid decomposition over complex metal oxide catalysts, Int. J. Hydrogen Energy 34 (9) (2009) 4065–4073.
[33] A. Balla, C. Marcu, D. Axente, G. Borodi, D. Lazăr, Catalytic reduction of sulfuric acid to sulfur dioxide, Cent. Eur. J. Chem. 10 (6) (2012) 1817–1823.
[34] D. Fleig, Experimental and modeling studies of sufur-based reactions in oxy-fuel combustion, Chalmers University of Technology (2012).
[35] C. Technology, C. Technology, I. Boletini, F. Technology, Characterisation of Karaceva bentonite by chemical composition, granulometric analysis and mossbauer spectroscopy Mehush Aliu, Mensur Kelmendi, Luljeta Pula-Beqiri, Milaim Sadiku Sadija Kadriu, J. Chem. Technol. Metall. 53 (3) (2018) 480–485.
[36] M. Chouafa, A. Idres, A. Bouhedja, K. Talhi, Chemical treatment of Kaolin. Case study of Kaolin from the Tamazert – Jijel Mine, Min. Sci. 22 (2015) 171–180.
[37] F.G. Colina, S. Esplugas, J. Costa, High-temperature reaction of kaolin with sulfuric acid, Ind. Eng. Chem. Res. 41 (17) (2002) 4168–4173.
[38] A.K. Panda, B.G. Mishra, D.K. Mishra, R.K. Singh, Effect of sulphuric acid treatment on the physico-chemical characteristics of kaolin clay, Colloids Surf. A Physicochem. Eng. Asp. 363 (1–3) (2010) 98–104.
[39] T.F.H. Mohamed, S.S. Abd, E. Rehim, M.A.M. Ibrahim, Improving the corrosion behavior of ductile cast iron in sulphuric acid by heat treatment, Der. Chem. Sin. 8 (1000) (2017) 513–523.
[40] E. Härkönen, et al., Corrosion protection of steel with oxide nanolaminates grown by atomic layer deposition, J. Electrochem. Soc. 158 (11) (2011) C369.
[41] B.J.P. Bennett, Corrosion resistance of selected ceramic materials to sulfuric acid, Estados Unidos, Washington D.C., 1986.
[42] L. Stoch, "Chemical reactions of clay minerals and their utilization." Proc. 9th Int. Clay Conf., Strasbourg, 1989, V.C. Farmer, Y. Tardy (eds.), Sci. Géol., Mém., V(89), 1990, p. 111–120.
[43] L. Bieseki, F. Bertell, H. Treichel, F.G. Penha, S.B.C. Pergher, Acid treatments of montmorillonite-rich clay for Fe removal using a factorial design method, Mater. Res. 16 (5) (2013) 1122–1127.
[44] A. Kunwadee Rangsriwatananon Chaisena, Effects of thermal and acid treatments on some physico-chemical properties of Lampang diatomite, J. Sci. Technol. 11 (6) (2004) 289–299.
[45] S. Musić, N. Filipović-Vinceković, L. Sekovanić, Precipitation of amorphous SiO_2 particles and their properties, Braz. J. Chem. Eng. 28 (1) (2011) 89–94.
[46] C.Y. Chen, G.S. Lan, W.H. Tuan, Microstructural evolution of mullite during the sintering of kaolin powder compacts, Ceram. Int. 26 (2000) 715–720.
[47] Y. Li, K. Liang, B. Xu, J. Cao, Crystallization mechanism and microstructure evolution of Li_2O–Al_2O_3–SiO_2 glass-ceramics with Ta_2O_5 as nucleating agent, J. Therm. Anal. Calorim. 101 (3) (2010) 941–948.
[48] J.W. von Goethe, Formation and transformation (1806), Comput. Des. Think. 338 (November) (2011) 335–338.
[49] G.G. Berhe, V.D.R. Alberto, B. Tadesse, A. Yimam, G. Woldetinsae, Decomposition of the Kenticha mangano-tantalite ore by HF/H_2SO_4 and KOH fusion, Physicochem. Probl. Miner. Process. 54 (2) (2018) 406–414.